MATERIALS PHYSICS AND MECHANICS RESEARCH ARTICLE

Submitted: August 7, 2023 **Revised: September 20, 2023** **Accepted: October 27, 2023**

Comprehensive studies of pipes metal to identify the causes of failure in the gas pipeline of the gas lift system of an oil and gas condensate field

A.M. Kunakova [1], V.A. Svintsov [2], V.A. Olenev [2], D.A. Gogolev [1], L.R. Sayfutdinova [1], M.S. Solodovnikova [1]✉

[1] Gazprom Neft PJSC, St. Petersburg, Russian Federation

[2] Gazpromneft-Orenburg LLC, Orenburg, Russian Federation

✉ solodovnikova.ms@gazprom-neft.ru

ABSTRACT

The results of a comprehensive study of pipes metal to identify the causes of failure in the gas pipeline of the gas lift system of an oil and gas condensate field transporting gas with a high content of carbon dioxide and hydrogen sulfide are presented. The research program included visual assessment of the pipe surface, metallographic, mechanical, electrochemical tests, determination of the chemical composition of steel and deposits. According to the results of the studies, it was established that the destruction of the pipeline was the result of thinning of the pipeline wall along the upper generatrix with the subsequent appearance of a crack up to the through outlet to the outside. Gas pipelines subjected to corrosion along the upper generatrix require a systematic approach to prevent failures.

KEYWORDS

studies of pipes metal • causes of failure in the gas pipeline • corrosion • corrosion along the upper generatrix causes of failure analysis • gas pipeline • top of the line corrosion

Citation: Kunakova AM, Svintsov VA, Olenev VA, Gogolev DA, Sayfutdinova LR, Solodovnikova MS. Comprehensive studies of pipes metal to identify the causes of failure in the gas pipeline of the gas lift system of an oil and gas condensate field. *Materials Physics and Mechanics*. 2024;52(4): 172–182. http://dx.doi.org/10.18149/MPM.5242024_15

Introduction

At present, the issue of safety of pipeline transportation facilities is given special attention [1,2]. Numerous studies prove that underground gas pipelines, operated under normal conditions, remain in satisfactory condition for several decades [3,4]. This is facilitated by systematic monitoring of the condition of gas pipelines and timely response to the appearance of corrosion-hazardous factors [5–8]. However, for a number of reasons, their premature failure may occur due to the destruction of the pipes metal [9].

Defects in such gas pipelines are often caused by corrosion and mechanical damage, the determination of the location and nature of which is associated with certain difficulties and material costs [10]. Most gas pipelines are laid underground, which complicates visual inspection limited only to the outer surface of the pipe [11–13]. Therefore, when accidents occur on gas pipelines, scientific and technical and research centers direct great efforts to investigate the causes of the incident, monitor the condition of the pipe surface and prevent further accidents [14–16].

Reduced reliability of the gas pipeline network leads not only to an increased risk of safe gas transportation, but also to possible socio-economic consequences associated with emergencies arising in case of accidents in such networks [17].

This article presents an approach to investigating one of a series of failures of a gas pipeline at a field in the Orenburg region, Russia. The failure was a pipe rupture, accompanied by a release of hydrogen sulfide-containing gas.

Three hypotheses were considered among the main causes of the incident:

1. non-compliance of the gas pipeline operating conditions with technical and design solutions;
2. poor quality of the pipe material;
3. high aggressiveness of the environment that promotes to metal corrosion [14].

Materials and Methods

The research program included analysis of field data, visual assessment of pipe samples, analysis of chemical composition of steel and corrosion deposits, metallographic, mechanical and electrochemical tests, and hydrodynamic calculations.

Laboratory tests were conducted on two pipe fragments (No. 2 and No. 5) subjected to general and pitting corrosion, cut from the gas pipeline from one direction. Pipe fragment No. 5 was cut from the failure site. To assess the quality of the pipe material, the composition and structure of the metal were studied, hardness and microhardness were determined. The chemical composition of steels was determined using an Iskroline 100 emission spectrometer in accordance with GOST R 54153-2010 [18]. Samples for metallographic studies of pipe fragments were cut out in the longitudinal direction. Contamination with non-metallic inclusions (NMIs) was assessed without decoding their chemical composition. To assess the microstructure, the samples were etched using a 4 % solution of nitric acid in ethanol; the studies were performed using optical metallography methods at ×100 and ×500 magnification on a Reichert-Jung MeAF-3A microscope.

The hardness of pipe fragments was determined on transverse samples. Hardness measurements were made using the Brinell method in accordance with GOST 9012-59 [19]. To determine the mechanism of crack formation, the appearance of the fracture was analyzed using a scanning electron microscope. The chemical composition of corrosion products was determined using raster scanning spectroscopy on a Zeiss Supra 55-VP electron microscope with an energy-dispersive X-ray spectrometer attachment.

To assess the corrosion resistance in pipeline sections subjected to general and local corrosion, one sample was cut from each pipe by electrochemical testing, one from a place subject to general corrosion, and one from a place with pitting corrosion.

The surface of the samples was ground using abrasive paper with a grit of 180–1200 and polished to 1 μm using polishing cloths on a Buehler EcoMet 4 grinder polisher machine. Grinding and polishing were performed until a homogenous mirror surface was achieved. Before testing, the surface of the samples was degreased using an alcohol-containing solution and acetone. The tests were performed using a Princeton Applied Research VersaSTAT potentiostat.

Electrochemical tests were performed in a closed hermetic cell with the possibility of creating flow movement. As a working electrolyte a 5 % solution of sodium chloride NaCl prepared with distilled water with a natural pH = 6.2 was used.

The studies on the prepared samples were performed in three stages. In the first two stages, the studies were performed in the working electrolyte in an aerated medium and in a flow. In the first stage, measurements were performed on samples with deposits and corrosion products, in the second stage – on ground and polished samples. The third stage of the studies was performed on ground and polished samples in the medium of electrolyte solution saturated with carbon dioxide and hydrogen sulfide. For this, the prepared electrolyte in a sealed flask was deaerated with nitrogen for 30 min, then saturated with H_2S for 10 minutes and CO_2 (50% mixture with nitrogen) for 2 min.

All tests were performed at ambient temperature (~23 °C). The flow in the cell was created by continuously stirring the electrolyte solution with a magnetic stirrer at a stirrer rate of 600 rpm. Under the condition that the length of the stirring anchor was about 25 mm, the flow rate was ~ 1.5 m/s. The equilibrium corrosion potential (E_{cor}) was measured for 55 min (3300 s). Then, anodic polarization was performed in the potentiodynamic mode in the potential range from -200 to 200 mV relative to the corrosion potential E_{cor} with a sweep rate of 0.16 mV/s and a polarization curve was obtained.

The polarization curves were used to determine the corrosion current density j_{cor} using a graphical method, on the basis of which the theoretical corrosion rate was calculated using Eq. (1), derived from Faraday's laws of electrolysis in accordance with ASTM G59-97 [20] and ASTM G102-89 [21]:

$$CR = C_1 \frac{j_{cor}}{\rho} EW, \quad (1)$$

where CR is a corrosion rate, mm/year, C_1 is a correction factor, $C_1 = 3.27 \cdot 10^{-3} \frac{\text{mm g}}{\mu\text{A cm year}}$, J_{cor} is a corrosion current density, μA/cm^2, $\rho_{steel} \approx 7.8$ g/sm^3.

The equivalent weight (EW) was calculated by:

$$EW = \frac{1}{\sum \frac{n_i g_i}{W_i}}, \quad (2)$$

where n_i is the valence of the i-th element, W_i is the atomic weight of the i-th element, g_i is the mass fraction of the i-th element.

In this work, the EW was taken as average for carbon steels and equal to 27.92 according to ASTM G102-89 [21].

Results and Discussion

The studies on determination of chemical composition of the pipes metal were conducted to confirm the material's compliance with regulatory and technical documentation. The results of determination of the chemical composition are presented in Table 1.

The conducted study showed that the chemical composition of the metal of fragment No. 2 corresponds to the composition of steel grade 25 according to GOST 1050-2013 [22], and the chemical composition of the metal of fragment No. 5 corresponds to steel grade 20 according to GOST 1050-2013.

Table 1. Chemical composition of pipe fragments

Grade	Component mass fractions, %									
	C	Si	Mn	Cr	Ni	Cu	Mo	Al	S	P
No. 2	0.266	0.210	0.550	0.090	0.130	0.170	0.030	0.030	0.006	0.008
No. 5	0.235	0.270	0.530	0.020	0.043	0.006	-	0.040	0.013	0.010
Steel 20	0.170-0.240	0.170-0.370	0.350-0.650	⩽0.250	⩽0.300	⩽0.300	-	-	⩽0.035	⩽0.030
Steel 25	0.220-0.300	0.170-0.370	0.350-0.650	⩽0.250	⩽0.300	⩽0.300	-	-	⩽0.035	⩽0.030

Based on the results of the conducted metallographic tests, it was established that the NMI contamination of all pipe fragments (No. 2 and No. 5) does not exceed 1 point according to the comparison scales of GOST 1778-2022 [23]. This means that the size and number of such inclusions do not have a noticeable effect on the mechanical characteristics of the pipe fragments. The microstructure of fragments No. 2 and No. 5 outside the crack zone is shown in Fig. 1.

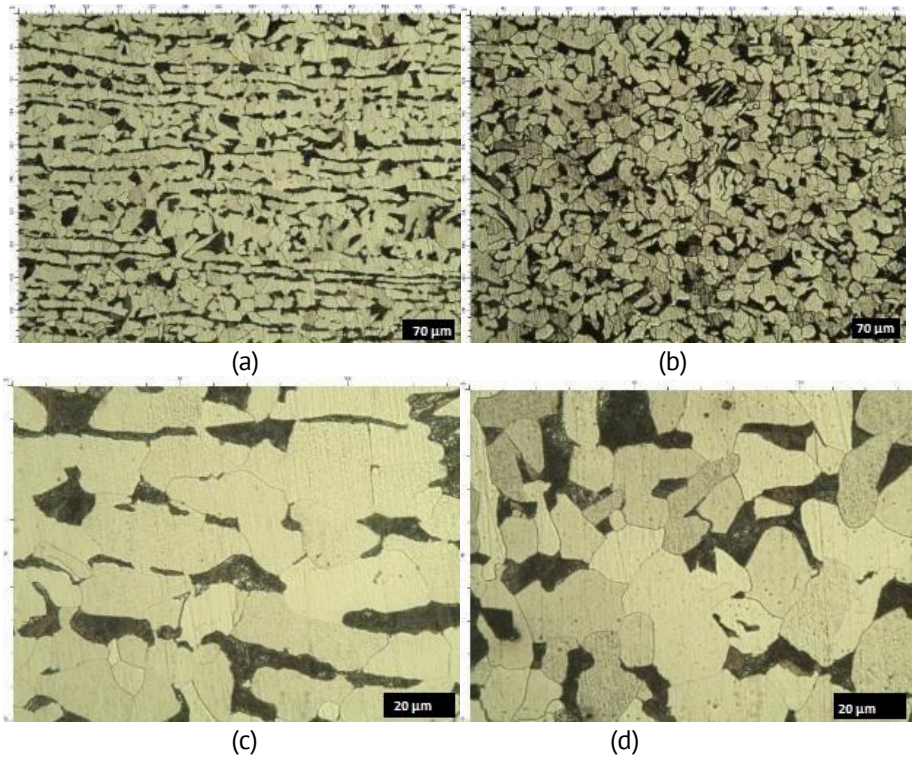

Fig. 1. Microstructure of fragments No. 2 (a,c) and No. 5 (b,d)

The microstructure of the studied fragments No. 2 and No. 5 is a combination of ferrite and pearlite. The ferrite grains in the microstructure of fragment No. 2 are more elongated along the rolling direction, compared to the structure of fragment No. 5. The distribution of microhardness along the cross-section of the pipe fragments No. 2 and No. 5 is shown in Fig. 2. The microhardness of fragments No. 2 and No. 5 is at the same level.

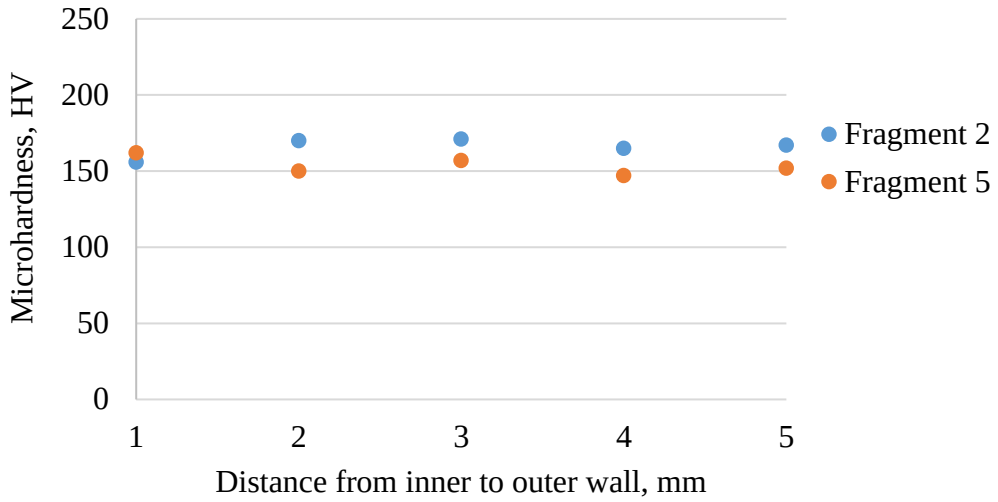

Fig. 2. The distribution of microhardness along the cross-section of the pipe

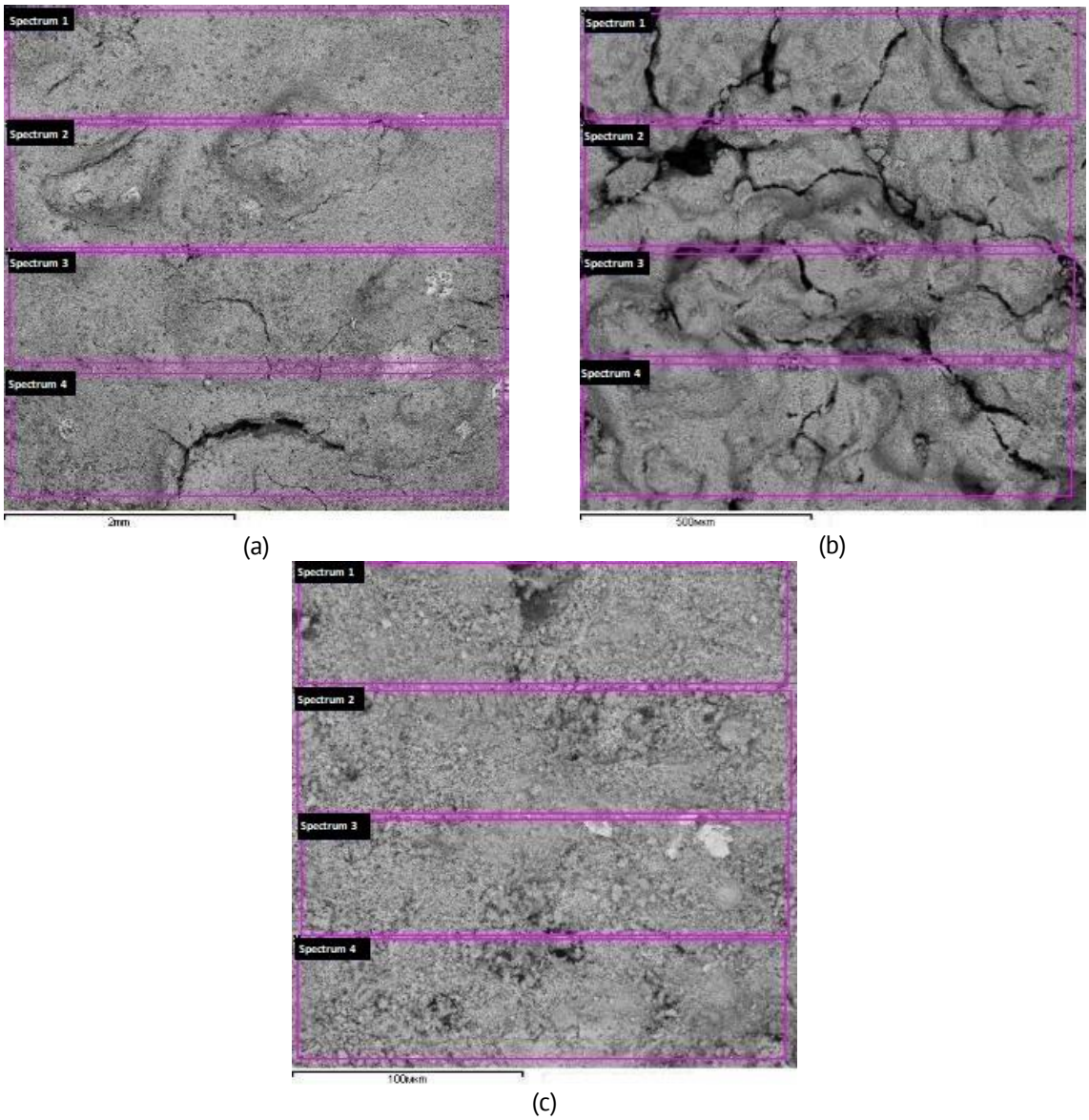

Fig. 3. Corrosion products of the studied fragments: (a) fragment No. 2, (b) fragment No. 5, (c) fragment No. 5 (in the crack area)

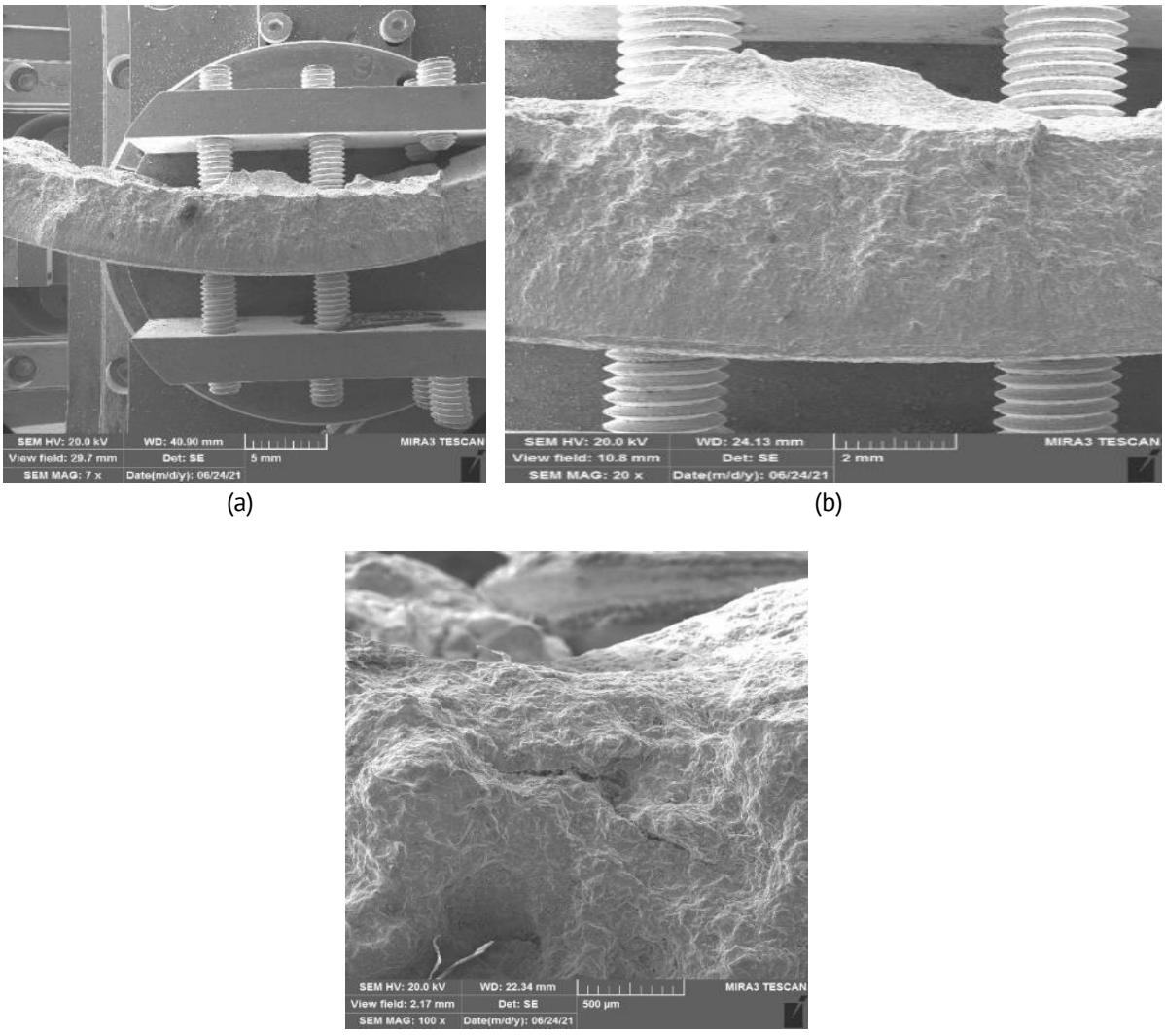

Fig. 4. External appearance of the fracture surface: (a) side view, (b) surface view, (c) fracture nature

The microhardness level in the crack zone is higher compared to fragments No. 2 and No. 5 outside the crack zone. The obtained hardness values are shown in Table 2. The table shows that the hardness values of fragment No. 2 slightly exceed the hardness value of fragment No. 5.

Table 2. Obtained hardness values

No. of a fragment	Hardness, HB				
	1	2	3	4	5
2	156	170	171	165	167
5	162	150	157	147	152

Thus, according to the research results, the hypothesis about the poor quality of the pipe material turned out to be erroneous. To clarify the mechanism of crack formation, an analysis of the appearance of the destruction was performed using a scanning electron microscope. Visual inspection of the studied pipe samples revealed that the inner surface of the pipe fragments was covered with corrosion deposits, there was a through crack on

pipe fragment No. 5, the minimum wall thickness of the pipe in the crack area was 5.83 mm (with an initial wall thickness of 8 mm). To test the hypothesis of destruction occurrence due to corrosion, the chemical composition of the deposits was determined. The corrosion products are shown in Fig. 3.

The results of determining the chemical composition of the deposits revealed that the corrosion products of the studied fragments No. 2 and No. 5 mainly consist of Fe, O and S. In the crack area of pipe fragment No. 5, the corrosion products mainly include the elements Fe, Mn, Si, C, O, S and Ca.

After the removal of the corrosion products from the inner surface of the pipe fragment No. 5 and examination of the fracture surface using a scanning electron microscope, it was determined that the crack originated from the inner surface of the pipe, in addition, the presence of secondary cracks was revealed. Figure 4 shows the appearance of the fracture surface.

Among the possible hypotheses of crack occurrence, the following were identified: hydrogen sulfide stress corrosion cracking due to the presence of hydrogen sulfide in the environment, cracking in the weld zone, thinning with reaching critical values, and local hydrogenation of the metal.

In hydrogen sulfide stress corrosion cracking, destruction occurs in the most stressed direction, i.e. along the pipeline, since the stress in this direction is 2 times higher than in the transverse direction, but the analysis results did not confirm this. In addition, in hydrogen sulfide stress corrosion cracking, crack development is possible at the site of a local defect, but metallographic studies showed that there is no local defect in the crack area.

The analysis results showed that the crack was formed in a section without a weld. Thus, the most likely mechanism for crack occurrence is local thinning of the metal up to critical values (25 %) with possible hydrogenation as a result of H^+ ions entering through corroded caverns.

The results of electrochemical tests revealed that the corrosion rates of samples with corrosion deposits are lower than the corrosion rates of ground samples. This is probably due to the fact that the corrosion products formed on the pipe surface (during general and local corrosion) slow down the further development of corrosion processes. While the ground, bare metal surface actively reacts with the aggressive corrosive environment.

A similar trend is observed among the values of corrosion potentials: the corrosion potentials of samples with corrosion deposits have higher values compared to samples with a ground surface. It is known that the higher (greater) the values of the equilibrium corrosion potential E_{corr}, the greater the corrosion resistance of the sample in a given environment. Samples with a ground surface have lower corrosion potentials compared to samples with deposits and, accordingly, have lower corrosion resistance.

Comparing the values of corrosion potentials and corrosion rates of pipe samples with general corrosion and local (pitting) corrosion, it can be noted that the corrosion rates at the pitting site are higher, and the corrosion potential values are lower. The metal at the pitting site has an uneven surface with multiple depressions. These defects become sites for the development of further pitting corrosion during electrochemical studies, even despite the presence of corrosion products. This probably explains the increased

values of corrosion rates of samples with the pitting type of destruction compared to samples with continuous corrosion.

Metal samples subjected to general corrosion have lower corrosion rates and higher corrosion potential values due to the fact that there are no obvious depressions or defects on the surface that could serve as sites for the development of local corrosion. The surface of the sample is protected from active dissolution by homogeneously formed corrosion products. Gas saturation with carbon dioxide and hydrogen sulfide has a negative effect on the corrosion resistance of the samples. The corrosion rate of all similar ground samples under conditions of gas saturation with CO_2 and H_2S increases by approximately 25–30 % compared to the results obtained on ground samples under aeration conditions.

It is important to note that the corrosion rates of ground metal samples from fragment No. 2 (steel 25) under both free aeration and CO_2 and H_2S gas saturation conditions are lower than the corrosion rates of ground metal samples from fragment No. 5 (steel 20). Also, the corrosion potential values of the samples from fragment No. 2 under both free aeration and CO_2 and H_2S gas saturation conditions are higher than the values of potentials of the samples from fragment No. 5, respectively, pipe fragment No. 2 (steel 25) has a higher corrosion resistance than pipe fragment No. 5 (steel 20).

The results of the hydrodynamic calculation revealed that the flow velocity in the direction of failure is 0.4–0.7 m/s. The flow regime is laminar, the flow is low-speed two-phase. On the inner surface of the pipeline, it is possible to visually determine the liquid-gas phase boundary by characteristic deposits, from which it is possible to assess the filling of the pipeline with liquid, which is 8–12 %. Thus, the liquid does not contact the upper inner surface of the pipeline.

Conclusion

Since the transported liquid contains CO_2 (2.17 %) and H_2S (5.42 %), the mechanism of combined carbon dioxide and hydrogen sulfide corrosion is active. The ratio of the partial pressure of carbon dioxide to the partial pressure of hydrogen sulfide is 0.39, therefore, the mechanism of hydrogen sulfide corrosion prevails [24].

According to the results of the analysis of corrosion products taken from the inner surface of the studied pipe fragments, the deposits mainly consist of iron and sulfur elements, which indicates that the corrosive agent is hydrogen sulfide contained in the transported wet gas.

Visual inspection of pipe fragments No. 2 and No. 5 revealed localized destruction on the inner surface, as well as characteristic corrosion products formed due to the effects of carbon dioxide and hydrogen sulfide. Localized corrosion is observed along the upper generatrix; the wall thickness in the area of destruction is 5.5 mm. The surface of the pipeline along the lower generatrix is smooth and has the greatest residual thickness of 7.72 mm (with an initial thickness of 8 mm).

Corrosion along the upper generatrix of the pipeline is observed under laminar stratified conditions, in which the liquid flowing along the bottom of the pipeline does not contact the upper generatrix [25–28]. The phenomenon consists of condensation of water vapor on the pipeline wall along the upper generatrix. Condensed water has a pronounced pH shift toward the acidic side due to the dissolution of CO_2 and H_2S in it.

Thus, the main cause of accelerated corrosion of pipe fragment No. 5 is the effect of wet gas containing carbon dioxide and hydrogen sulfide, which contribute to a decrease in the pH of the environment. As a result of corrosion, there was a thinning along the upper generatrix of the pipe up to a critical value, after which the initiation and growth of a crack to its through exit to the outside was observed [29].

As an emergency measure to protect gas pipelines of the gas lift system, it is recommended to use a corrosion inhibitor [30], which should be introduced using a spray nozzle or by periodic pumping in the form of a plug. The inhibitor should have high efficiency in the gas phase.

According to the conducted literature analysis [24], gas pipelines with flow rates of up to 3 m/s are at risk of possible corrosion along the upper generatrix of the pipe. To prevent water condensation along the upper generatrix, it is necessary to flush with liquid or increase the velocity of the transported gas. Thus, to reduce the localization of the corrosion process, an increase in gas flow rate is required to switch to the annular mode of a two-phase flow. If there is no possibility to increase the gas flow rate, it is recommended to reduce the diameter of the pipelines.

References

1. Izgagina TYu. Some security issues in pipeline transport. *Juridical Journal of Samara University*. 2021;7(3): 91–101. (In Russian)
2. Makhutov NA, Lisin YV, Fedota VI, Aladinskii VV. Safety and Risk Assessment of Critically and Strategically Important Pipelines. *Science and Technologies: Oil and Oil Products Pipeline Transportation*. 2011;2: 6–13. (In Russian)
3. Kharionovsky VV. Service life of gas pipelines with long operation periods. *Gas Industry Journal*. 2017;5(752): 56–61. (In Russian)
4. Makhutov NA, Lebedev MP, Bolshakov AM, Zakharova MI. Features of occurrence of emergency situations on gas pipelines in the North. *Bulletin of the Russian Academy of Sciences*. 2017;87(9): 858–862. (In Russian)
5. Goldobina LA. Ways to reduce accident rates on underground pipelines of municipal services. *Innovation processes in the service sector: problems and prospects*. 2010;2: 296–300. (In Russian)
6. Glazkov VI, Zinevich AM, Kotik VG et al. *Corrosion protection of extended metal structures*. Moscow: Nedra; 1969. (In Russian)
7. Krasnoyarsky VV. *Underground corrosion of metals and methods of combating it*. Moscow: Publishing House of the Ministry of Public Utilities of the RSFSR, 1962. (In Russian)
8. Roberge PR. *Handbook of corrosion engineering*. USA: McGraw-Hill, 2000.
9. Lubchik AN, Krapivsky EI, Bolshunova OM. Prediction of the technical status of pipeline based on analysis. *Journal of Mining Institute*. 2011;192: 154–157. (In Russian)
10. Poezzhaeva EV, Fedotov AG, Zaglyadov PV. Development of a robot for pipeline inspection. *Young Scientist*. 2015;16: 218–222. (In Russian)
11. Kuklin AA, Bushmeleva KI. Expert system for complex diagnostics of the technical condition of gas transportation network facilities. In: *Proceedings of the International Symposium "Reliability and Quality"*. 2011. p.46–49. (In Russian)
12. Sedak VS, Nesterenko SV, Slatova ON, Bronevskij YuF. Analysis of gas leaks and causes of stress-corrosion damage in underground pipelines. *Municipal Economy of Cities*. 2013;110: 182–188. (In Russian)
13. Goldobina LA, Orlov PS. Analysis of the corrosion destruction causes in underground pipelines and new solutions for increasing corrosion steel's resistance. *Journal of Mining Institute*. 2016;219: 459–464. (In Russian)
14. Savonin SV, Moskalenko AV, Tyunder AV. Analysis of the main causes of accidents that occurred on gas pipelines. *Engineering protection*. 2015;6(11): 52–57. (In Russian)
15. Vorobiev VA. Reliability of existing pipeline transport systems and ways to improve it. In: *Work program of the 3rd Congress of Oil and Gas Industrialists of Russia*. TPPRB; 2001;3: 33–39. (In Russian)
16. Gafarov NN. Failure analysis and assessment of the residual life of pipelines and equipment at the Orenburg oil and gas condensate field. *Abstracts of the report of the 3rd International Conference "Pipeline Diagnostics"*. 2001. (In Russian)
17. Balandina EA, Timoshenko SV. Assess whether to use hardware-software complex tele to reduce the risk of accidents on gas distribution item and setting. *Scientific review. Technical sciences*. 2015;1: 65–66. (In Russian)

18. Interstate Council for Standardization, Metrology and Certification (ISC). *Steel. Method of atomic emission spectral analysis*. GOST R 54153-2010. 2012.
19. Interstate Council for Standardization, Metrology and Certification (ISC). *Metals. Method of Brinell hardness measurement*. GOST 9012-59. 2007.
20. American Society for Testing and Materials (ASTM International). *Standard Test Method for Conducting Potentiodynamic Polarization Resistance Measurements*. ASTM G59-97. 2020.
21. American Society for Testing and Materials (ASTM International). *Standard Practice for Calculation of Corrosion Rates and Related Information from Electrochemical Measurements*. ASTM G102-89. 2015.
22. Interstate Council for Standardization, Metrology and Certification (ISC). Metal products from nonalloyed structural quality and special steels. General specification. GOST 1050-2013. 2015. 36 p.
23. Interstate Council for Standardization, Metrology and Certification (ISC). Steel and alloy metal products. Metallographic methods for the determination of nonmetallic inclusions. GOST 1778-2022. 2023.
24. Singer M. Top of the line corrosion in sour environment – study of the controlling parameters. *Journal of Materials Science*. 2011;18(80): 1–10.
25. Svenningsen G, Kvarekvål J. Sour Top of Line Corrosion. *Corrosion*. 2018; NACE-2018-10964.
26. Gunaltun YM, Larrey D. Correlation of cases of top of line corrosion with calculated water condensation rates. *Corrosion*. 2000; NACE-00071.
27. Jenkins A, Gilbert I. Development of a top-of-line corrosion inhibitor and a top-of-line corrosion test method. *Corrosion*. 2012; NACE-2012-1275.
28. Al-Moubaraki AH, Obot IB. Top of the line corrosion: causes, mechanisms, and mitigation using corrosion inhibitors. *Arabian Journal of Chemistry*. 2021;14(5): 103116.
29. McCafferty E. *Introduction to corrosion science*. NY: Springer New York, 2010.
30. Srinivasan S, Jangama VR, Kane RD. Prediction of corrosivity of multiphase CO_2/H_2S systems. *Proceedings of EUROCORR'97*. 1997;1: 35.